Solving Optimal Power Flow Problem of Power System Based on Archimedes Optimization Algorithm

Jun-Hua Zhu, Jie-Sheng Wang *, Xing-Yue Zhang

Abstract— **The fundamental purpose of optimal power flow in power system is to improve the economic indexes and stability indexes such as generation cost and voltage deviation on the premise of satisfying the operation constraints and supply and demand balance. The model of the optimal power flow problem is established by taking the system power balance, generator set output limit and transformer tap as constraints. In this experiment, Archimedes optimization algorithm (AOA) is used to solve OPF problem with IEEE-30 bus system. Total generation cost, active power loss, voltage stability and bus voltage offset are selected as the evaluation indexes in the OPF problem. Then the experimental data of AOA are compared with several meta-heuristic algorithms, so as to test and verify the excellent performance of AOA. Simulation results show that AOA can be used as a powerful alternative technique to solve the OPF problem.**

Index Terms—**optimal power flow; archimedes optimization algorithm; constrained optimization; power system**

I. Introduction

OPTIMAL power flow (OPF) is designed to optimize generation costs or other reliability indicators. OPF changes the power flow of the whole power network by regulating the control variables when the system and equipment constraints are satisfied. Like traditional power flow calculation, OPF is closely related to the running status of the entire system, including the voltage level of every bus and the active and reactive power injected into each node. But unlike traditional power flow calculations, OPF is suitable for an unconstrained network with plural control variables, and there can be multiple solutions. Therefore, OPF performs several power flow iterations to modify control variables to optimize fuel cost, voltage stability and other indicators. The OPF is a highly nonlinear and non-convex optimization problem, which not only has many constraints, but also can contain both continuous and discrete control variables[1]. Ref. [2-4] has studied OPF problem by using classical techniques in operations research, and the solution methods include linear programming, nonlinear programming, Newton method and gradient method, etc. The OPF problem is relatively complex and computation scale is large. The solutions obtained by the above optimization methods are often local optimal solutions, so these optimization methods can not deal with the OPF problem well. Due to the limitation of traditional mathematical optimization methods, many researchers have turned their focus to swarm intelligence optimization algorithms that perform well in many fields. Ref. [5] improved the grey wolf optimizer, named CS-GWO, which added horizontal and vertical crossover operators for optimization, and achieved good results in OPF problems. Ref. [6] improved the whale optimization algorithm, named EWOA, and added two hunting methods to make the predation process more effective. The algorithm is simulated in four OPF test systems, and the promising results are obtained especially in the case of multiple targets. In Ref. [7], the constraint processing technology and adaptive penalty are applied to the setting of static penalty function in OPF problem, and satisfactory experimental results are obtained. In Ref. [8], Sayah and Zehar improved the differential evolution algorithm to deal with the OPF for thermal power units including non-smooth and non-convex fuel cost functions. The mutation operator is modified effectively to ensure both the convergence rate of the curve and the accuracy of the solution. In Ref. [9], Elattar et al. used the modified JAYA algorithm to deal with the test system with new energy, and obtains satisfactory results. In Ref. [10], Zhang solved the OPF problem by using a small-population hybrid particle swarm optimization method (HPSO-SP). In Ref. [11], Mahdad and Srairi adopted adaptive partitioning flower pollination algorithm (APFPA) to smoothly deal with the OPF problem by taking into account of main generator set failures. In Ref. [12], Bentouati et al. added chaotic behavior to salp swarm algorithm (SSA) to deal with the OPF problem.

Recently, Fatma A. Hashim proposed a new meta-heuristic algorithm: archimedes optimization algorithm (AOA) [13]. AOA is inspired by Archimedes' law, a law of hydro-statics that states that if an object dip into liquid, it will experience upward buoyancy equal to the force of gravity on the liquid it displaces. If the buoyant force on an object is equal to its own gravity, then the object will be stationary; If the buoyancy force on an object is less than its own gravity, then the object sinks. AOA shows good

Manuscript received June 22, 2022; revised November 2, 2022. This work was supported by the Basic Scientific Research Project of Institution of Higher Learning of Liaoning Province (Grant No. LJKZ0293), and the Project by Liaoning Provincial Natural Science Foundation of China (Grant No. 2019-ZD-0031).

Jun-Hua Zhu is a postgraduate student of School of Electronic and Information Engineering, University of Science and Technology Liaoning, Anshan, 114051, P. R. China (e-mail: zhujunhua1999@163.com).

Jie-Sheng Wang is a professor of School of Electronic and Information Engineering, University of Science and Technology Liaoning, Anshan, 114051, P. R. China (Corresponding author, phone: 86-0412-2538355; fax: 86-0412-2538244; e-mail: wang_jiesheng@126.com).

Xing-Yue Zhang is a postgraduate student of School of Electronic and Information Engineering, University of Science and Technology Liaoning, Anshan, 114051, P. R. China (e-mail: 2751159468@qq.com).

convergence and searching performance. This algorithm has been applied to distribution network reconstruction [14], wind speed prediction [15] and maximum power tracking operation of wind generators [16]. In this experiment, archimedes optimization algorithm is applied to deal with the optimal power flow problem of power system, and its better performance is verified.

II. Mathematical Model of Optimal Power Flow Problem

The purpose of OPF problem is to improve the selected economic index or stability index under the condition of satisfying the safe operation of all devices in power network. Mathematically, the most commonly used model of OPF problem is defined as Eq.(1).

$$\begin{aligned} &Minimize \quad f(x,y) \\ &s.t. \quad g(x,y)=0 \\ &\quad\quad h(x,y)\le 0 \end{aligned} \tag{1}$$

where, $f(x,y)$ represents the optimization index of power system; $g(x,y)$ stands for equality constraint. The inequality constraint is $h(x,y)$; The control variable is denoted by x, while the state variable is denoted by y. Its details are provided below.

A. Control Variables

Control variables can be adjusted during the proper functioning of the power network to change the running state of the system. They mainly include four categories, which are the power output of the generator, the voltage level of the generator bus, the tap position of adjustable transformer and the reactive power of the shunt capacitor.

$$x=[P_{G_2},...,P_{G_{NG}},V_{G_1},...,V_{G_{NG}},T_1,...,T_{NT},Q_{C_1},...,Q_{C_{NC}}] \tag{2}$$

The active power output by the generator is $P_{G_2},...,P_{G_{NG}}$; The size of the generator bus voltage is $V_{G_1},...,V_{G_{NG}}$; $T_1,...,T_{NT}$ is the setting of transformer tap; $Q_{C_1},...,Q_{C_{NC}}$ is the capacity of the parallel reactive capacitor; The number of generators, transformers and shunt capacitors are denoted by *NG*, *NT* and *NC* respectively.

B. State Variables

In the power system, there are some variables that change as control variables are adjusted. The names of these variables are state variables.

$$y=[P_{G_1},V_{L_1},...,V_{L_{NL}},Q_{G_1},...,Q_{G_{NG}},S_{l_1},...,S_{l_{Nl}}] \tag{3}$$

P_{G_1} is the active power input by the balancing node, which is used to balance the equality constraint of the active power shown in previous section. $V_{L_1},...,V_{L_{NL}}$ is the voltage of each load node in the power system. $Q_{G_1},...,Q_{G_{NG}}$ is the reactive power emitted by the generator and input into the grid. $S_{l_1},...,S_{l_{Nl}}$ is the power transmitted over the line. *NL* represents the total quantity of PQ nodes (load nodes). The total quantity of transmission lines is denoted by *Nl*.

C. Constraints Conditions

There are two types of constraints in the model of OPF problem, which are equality constraints on the power balance and inequality constraints on the normal operating range of each device. The purpose of equality constraints are to make the power generated by all generators in the system equal to the power consumed by load plus the power lost in the line, while inequality constraints are used to make the system run safely and stably. The most significant equality constraint are shown in Eq. (4) and Eq. (5):

$$\begin{aligned} P_{G_i}=P_{D_i}+V_i\sum_{j=1}^{NB}V_j[G_{ij}\cos(\delta_i-\delta_j) \\ +B_{ij}\sin(\delta_i-\delta_j)], \quad i=1,...,NB \end{aligned} \tag{4}$$

$$\begin{aligned} Q_{G_i}=Q_{D_i}+V_i\sum_{j=1}^{NB}V_j[G_{ij}\cos(\delta_i-\delta_j) \\ +B_{ij}\sin(\delta_i-\delta_j)], \quad i=1,...,NB \end{aligned} \tag{5}$$

Eq. (4) is the active power equation constraint, where P_{D_i} is the amount of active power consumed by the load. Eq. (5) is the reactive power equation constraint, where Q_{D_i} is the reactive power consumed by the load. *i* and *j* are both serial numbers of nodes, and in this equation, they are not equal. δ_i represents the phase angle of the *i*-th node; The inductance and conductance of transmission lines between nodes are denoted by B_{ij} and G_{ij}. *NB* indicates the number of nodes.

Inequality constraints are mainly constraints on the safe operation of the system, and the following four parts are considered in this paper.

(1) Generator constraints

$$P_{G_i}^{\min}\le P_{G_i}\le P_{G_i}^{\max}, \quad i=1,...,NG \tag{6}$$

$$Q_{G_i}^{\min}\le Q_{G_i}\le Q_{G_i}^{\max}, \quad i=1,...,NG \tag{7}$$

$$V_{G_i}^{\min}\le V_{G_i}\le V_{G_i}^{\max}, \quad i=1,...,NG \tag{8}$$

where, $P_{G_i}^{\min}$, $Q_{G_i}^{\min}$ and $V_{G_i}^{\min}$ are corresponding lower bounds; $P_{G_i}^{\max}$, $Q_{G_i}^{\max}$ and $V_{G_i}^{\max}$ are corresponding upper bounds.

(2) Compensator capacity constraints

$$Q_{C_j}^{\min}\le Q_{C_j}\le Q_{C_j}^{\max}, \quad j=1,...,NC \tag{9}$$

(3) Transformer constraints

$$T_K^{\min}\le T_K\le T_K^{\max}, \quad K=1,...,NT \tag{10}$$

(3) Safety constraints

$$V_{L_m}^{\min}\le V_{L_m}\le V_{L_m}^{\max}, \quad m=1,...,NL \tag{11}$$

$$S_{l_n}\le S_{l_n}^{\max}, \quad n=1,...,Nl \tag{12}$$

III. Optimization Objective Functions

The standard IEEE-30 bus system is selected as the simulation system of OPF in this paper, so as to verify the effectiveness of AOA. The system includes 6 generators and 4 transformers and Fig. 1 visually presents the structural framework of the 30-node system. Table 1 summarizes the

key information of the simulation system. This section describes the different optimization objectives, including fuel cost required by thermal power generation unit, active power loss during power transmission, voltage deviation of load node bus, voltage stability.

A. Objective Function 1 (Fuel Cost)

Fuel cost, also known as generation cost, is the most significant indicator of the OPF problem. After simplification, a quadratic equation is used to describe the relevance between fuel cost and generation power. Therefore, expression of the objective function is shown in Eq. (13):

$$f_{\text{cost}} = \sum_{i=1}^{NG} a_i + b_i P_{G_i} + c_i P_{G_i}^2 \tag{13}$$

where, a_i, b_i and c_i are the fuel cost coefficients of the unit output power of the i-th generator. The fuel cost factors for the six generators in the system are listed in Table 2.

B. Objective Function 2 (System Active Power Loss)

Power loss caused by the resistance in the transmission line is inevitable in power systems. The calculation formula of active power loss is shown in Eq. (14).

$$f_{Ploss} = \sum_{i=1}^{Nl} \sum_{j \neq i}^{Nl} G_{ij} [V_i^2 + V_j^2 - 2V_i V_j \cos(\delta_i - \delta_j)] \tag{14}$$

C. Objective Function 3 (Voltage Stability)

The problem of voltage stability is getting more and more attention in power system in that some countries' power grid collapsed because of node voltage fluctuation. In normal operation, The stability of a power network is defined as follows: after interference, all nodes in the system maintain the voltage within the safe range. When the large capacity unit is disconnected or the reactive power deficiency in the power network is large, which result in uncontrollable voltage drop, the voltage instability of the system will affect the safe operation of each device.

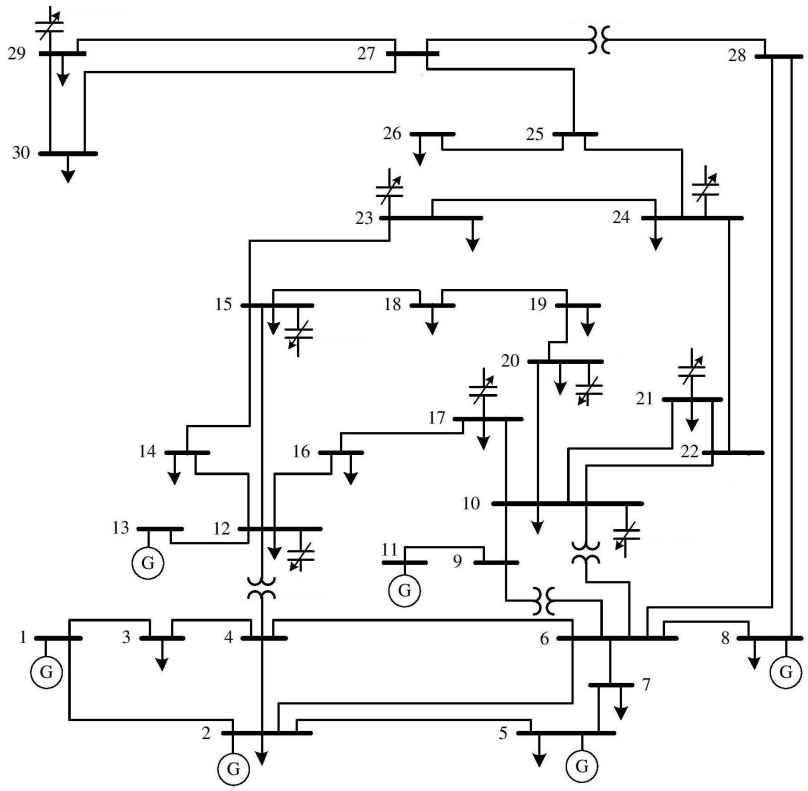

Fig. 1 Framework of standard IEEE-30 bus system.

TABLE 1. DETAILED DESCRIPTION OF STANDARD IEEE-30 BUS SYSTEM

Item	Quantity	Details
Bus	30	-
Branch	41	-
Thermal generator	6	Buses: 1 (swing), 2, 5, 8, 11 and 13
Shunt VAR compensation	9	Buses: 10, 12, 15, 17, 20, 21, 23, 24 and 29
On-load tap changer transformer	4	Branches: 11, 12,15 and 36
Control variables	24	-
Connected load	-	283.4 MW, 126.2 MVAr
Load bus voltage	24	[0.95 - 1.05] p.u.

TABLE 2. COEFFICIENT VALUES OF GENERATORS

Generator	Bus	*a*	*b*	*c*
G_1	1	0	2	0.00375
G_2	2	0	1.75	0.0175
G_3	5	0	1	0.0625
G_4	8	0	3.25	0.00834
G_5	11	0	3	0.025
G_6	13	0	3	0.025

As a crucial safety index, it is necessary to enhance the voltage stability of power grid to ensure that the electric energy is delivered to the load node safely. The L index of each bus needs to be calculated. The range of this index is [0,1]. When the line is unloaded, L index is 0. When a voltage collapse occurs, the L index is 1.

$$L_j = \left| 1 - \sum_{i=1}^{NG} F_{ji} \frac{V_i}{V_j} \right|, \quad j = 1, \ldots, Nl \tag{15}$$

where, i represents the serial number of the generator, j represents the serial number of the load bus. V_i and V_j are the bus voltages at their corresponding positions. F_{ji} can be computed by YBUS matrix. The L index of total load buses is calculated, and the crest value is used as the collectivity index of power network. Consequently, the system voltage stability index is defined as:

$$f_{Vstability} = \max(L_j), \quad j = 1, \ldots, Nl \tag{16}$$

D. Objective Function 4 (Voltage Deviation)

Voltage deviation can reflect the voltage quality of power system, and it is also a target used frequently in power system stability evaluation. The optimization index is the sum of the voltage deviations of all load buses in the power grid, as shown in Eq. (17).

$$f_{Vdeviation} = \sum_{m=1}^{NL} |V_{Lm} - 1.0|, \quad j = 1, \ldots, Nl \tag{17}$$

E. Objective Function 5 (Fuel Cost and Voltage Stability)

The goal is to optimize two indexes simultaneously: reducing the fuel cost of generators and improving the voltage stability of the grid. The linear weighting method is used to assign weights to the two indexes respectively and then add them. Finally, the sum value is taken as the optimization objective. This comprehensive objective equation can be described as:

$$f_{\text{cost-Lj}} = \left(\sum_{i=1}^{NG} a_i + b_i P_{G_i} + c_i P_{G_i}^2\right) + \lambda \times L_{j-\max} \tag{18}$$

where, the weight coefficient λ is set to 100 in this paper.

IV. Archimedes Optimization Algorithm

Archimedes Optimization algorithm (AOA) simulates the content of Archimedes' law of buoyancy. The algorithm assumes that multiple objects are simultaneously immersed in the same fluid, either in equilibrium or in motion. When in equilibrium, it means that the buoyancy force F_b on the object is equal to its gravity W_o. The motion state of different objects is also different, which needs to be further divided according to their respective forces.

$$\begin{aligned} F_b &= W_o \\ p_b v_b a_b &= p_o v_o a_o \end{aligned} \tag{19}$$

where, the density of the object is denoted by p, the volume of the object is denoted by v, and the gravity or acceleration of the object is denoted by a. b is the fluid, and o is the object in the fluid. This equation is deformed to obtain the following equation.

$$a_o = \frac{p_b v_b a_b}{p_o v_o a_o} \tag{20}$$

If the object is affected by external forces or colliding with other neighboring objects, the motion state of the object is as follows:

$$\begin{aligned} F_b &= W_o \\ W_b - W_r &= W_o \\ p_b v_b a_b - p_r v_r a_r &= p_o v_o a_o \end{aligned} \tag{21}$$

The initial population of AOA is also randomly generated, with each individual having different physical properties such as volume, followed by an iterative process. In the search process of AOA, physical properties such as density and acceleration of objects in the fluid are updated according to the following formula. When an object collides with another object, its acceleration changes. The fitness value of the population is calculated to evaluate the advantages and disadvantages of individuals. If the termination condition of the iteration is met, the iteration will end. Firstly, the initialization process is carried out by Eq. (22):

$$O_i = lb_i + rand \times (ub_i - lb_i), \quad i = 1, 2..., N \tag{22}$$

The upper and lower limits of the container in which the liquid resides are denoted by ub_i and lb_i. Eq. (23) is used to assign the density and volume of each body.

$$\begin{aligned} den_i &= rand \\ vol_i &= rand \end{aligned} \tag{23}$$

where, den_i and vol_i are D-dimensional vectors, and uniform distribution is used to produce a set of stochastic numbers with a range of [0,1]. Then finally initialize the acceleration with Eq. (24). During this process, the fitness value of each search agent was calculated, and the individual with the best value was chosen and recorded, which are denoted as x_{best}, den_{best}, vol_{best} and acc_{best}.

$$acc_i = lb_i + rand \times (ub_i - lb_i) \tag{24}$$

The volume and density of the object in the fluid are updated by Eq. (25) in the process of iterations.

$$\begin{aligned} den_i^{t+1} &= den_i^{t+1} + rand \times (den_{best} - den_i^t) \\ vol^{t+1} &= vol^{t+1} + rand \times (vol_{best} - vol_i^t) \end{aligned} \tag{25}$$

where, vol_{best} and den_{best} are the best volume and density in the current iteration process. $rand$ is a stochastic number in the range [0,1].

At the beginning, objects collide with each other in a fluid and change their original state. By late phase, objects are in relative equilibrium. In AOA, the transfer operator TF defined in Eq. (26) is used to achieve this function. TF can better transform the exploration part into the development part.

$$TF = \exp \frac{t - t_{\max}}{t_{\max}} \tag{26}$$

where, TF is small at the beginning of the iteration and grows to a maximum value of 1 at the conclusion of the iteration; t represents the present iteration and $t_{\max}$ represents the maximum iteration. The density factor d also controls the search process, making AOA change from a large area search to a local search in the iteration process.

$$d^{t+1} = \exp\left(\frac{t - t_{\max}}{t_{\max}}\right) - \frac{t}{t_{\max}} \tag{27}$$

When $TF \leqslant 0.5$, the object is in the global search stage, and different objects collide with each other. After the impact process, the stochastic volume and density are selected as the physical properties of the body, and acceleration of the body is obtained by Eq. (28).

$$acc_i^{t+1} = \frac{den_{mr} + vol_{mr} + acc_{mr}}{den_i^{t+1} \times vol_i^{t+1}} \tag{28}$$

where, den_i, vol_i and acc_i are the density, volume and acceleration of the i-th object respectively; den_{mr}, vol_{mr}, and acc_{mr} are the density, volume, and acceleration of random materials respectively.

When $TF > 0.5$, the object is in the local search stage, and different bodies don't hit each other. At this time, the acceleration of the bodies will be updated according to Eq. (29). acc_{best} is the best individual acceleration.

$$acc_i^{t+1} = \frac{den_{best} + vol_{best} + acc_{best}}{den_i^{t+1} \times vol_i^{t+1}} \tag{29}$$

Normalized acceleration. Use Eq. (30) to normalize the acceleration.

$$acc_{i-norm}^{t+1} = u \times \frac{acc_i^{t+1} - \min(acc)}{\max(acc) - \min(acc)} + l \tag{30}$$

where, u and l are 0.9 and 1 respectively, which are used for normalization. Guided by the position of the global optimal individual, if the object is farther away from it, the object will get greater acceleration, and it is the global search stage. When the object come near the global optimum value, it is in the local search stage.

Location updates. When AOA is in the exploration stage, $TF \leqslant 0.5$, then Eq. (31) is used to change the position of the object.

$$x_i^{t+1} = x_i^t + C_1 \times rand \times acc_{i-norm}^{t+1} \times d \times (x_{rand} - x_i^t) \tag{31}$$

where, C_1 is a search coefficient, which is set to 2 in this paper. On the contrary, if AOA is in the development stage, Eq. (32) is used to change the position of the object.

$$x_i^{t+1} = x_{best}^t + F \times C_2 \times rand \times acc_{i-norm}^{t+1} \times d \times (T \times x_{best} - x_i^t) \tag{32}$$

where, C_2 represents a search coefficient, which is set to 6 in this paper. The calculation formula of T is: $T = C_3 \times TF$, and T gradually becomes larger in the interval of $[C_3 \times 0.3, 1]$. F controls the displacement direction of the object through Eq. (33).

$$F = \begin{cases} +1, & if\ p \leq 0.5 \\ -1, & if\ p > 0.5 \end{cases} \tag{33}$$

where, $p = 2 \times rand - C_4$.

Calculate the fitness of every agent, and record the coordinate, density, volume and acceleration of the optimal solution, which are record as x_{best}, den_{best}, vol_{best}, acc_{best}.

V. Experimental Results and Analysis

IEEE-30 bus system is used as the test system in this section. And the Experiments considers generation cost, active power loss during power transmission, voltage stability and bus voltage deviation as target indexes. In this experiment, the population number N was set to 50, and the maximum iteration number was set to 600. The algorithm was compiled and run in MATLAB 2019b, and was independently run for 10 times under each objective function. In this experiment, particle swarm optimization (PSO) and coyote optimization algorithm(COA) were used as comparison. The load bus voltages obtained by AOA are shown in Fig. 2 and Table 3. The setting of control variables corresponding to the optimal results of every case is shown in Table 4. Fig. 3 describes the voltage distribution of the load bus of the IEEE-30 bus system corresponding to the optimal result of every objective function.

In Case 1, Fig. 2(a) shows that the optimal value of AOA has been approached at 200 iterations, indicating good convergence. The optimal value of AOA is better than that of PSO and COA. In addition, it is apparent from Table 3 that the optimal value of 800.5005 $/h was finally found without violating the constraints. Compared with the optimal index of artificial bee colony algorithm, adaptive real coded biogeography-based optimization algorithm and modified differential evolution algorithm, their results were 0.019%, 0.002%, and 0.234% lower respectively. The average value and maximum value of AOA are lower than those of other algorithms, showing better stability.

In Case 2, Fig. 2(b) shows that the optimal value of AOA was approached at 220 iterations, and the final active power loss was 3.1282 MW. The optimal value of AOA is better than that of PSO. In Table 3, the minimum value of active power loss is 3.1078 MW, which was obtained by ABC algorithm. Compared with the minimum value of 3.2008 MW of the improved genetic algorithm, the results of AOA have certain competitiveness.

In Case 3, Fig. 2(c) shows that the optimal value of AOA has been approached after 240 iterations, and the final voltage stability index L-index (Max) is 0.1252 p.u. The optimal value of AOA is better than that of PSO and COA. In Table 3, compared with the optimal value of the ABC algorithm and the ARCBBO algorithm, their results were reduced by 15.061% and 9.472% respectively. The average value and maximum value of AOA are lower than those of other algorithms, showing better stability.

In Case 4, Fig. 2(d) shows that the optimal value of AOA has been approached after 200 iterations, and the final bus voltage deviation is 0.0871 p.u. The optimal value of AOA is better than that of PSO and COA. In Table 3, this result is 6.652% and 5.435% lower than the optimal value of the gravity search algorithm and the ARCBBO algorithm. The

average value and maximum value of AOA are also lower than those of other algorithms.

In Case 5, Fig. 2(e) shows that the optimal value of AOA has been approached after 170 iterations. The optimal value of AOA is better than that of PSO and COA. In Table 3, compared with the moth swarm algorithm and MDE algorithm, the result of AOA was reduced by 0.215% and 0.313% respectively. The average value and maximum value of AOA are also lower than those of other algorithms.

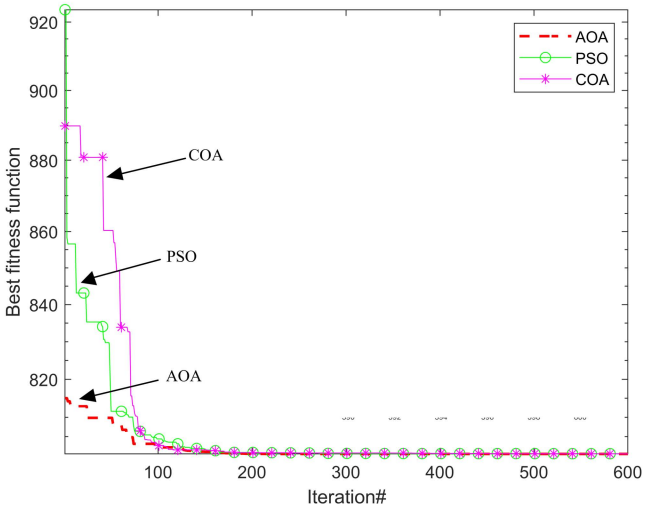

(a) Case 1

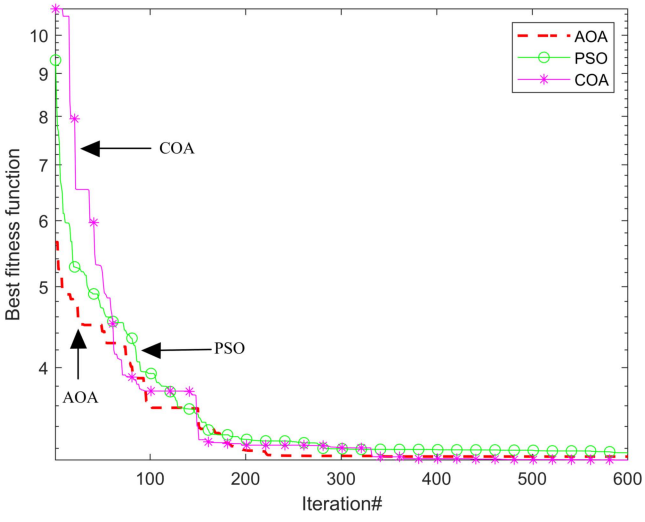

(b) Case 2

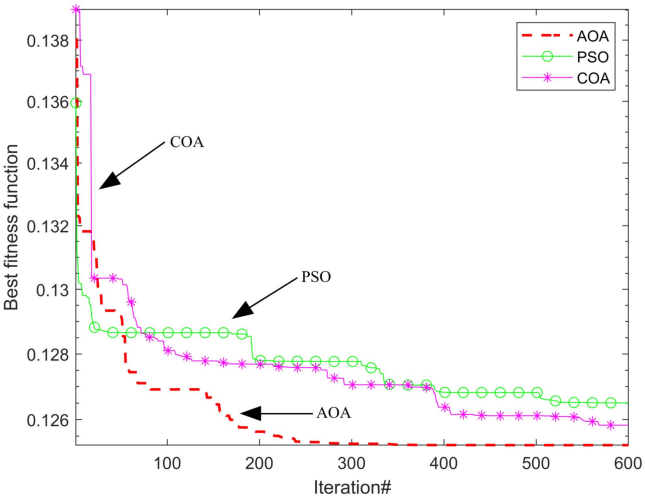

(c) Case 3

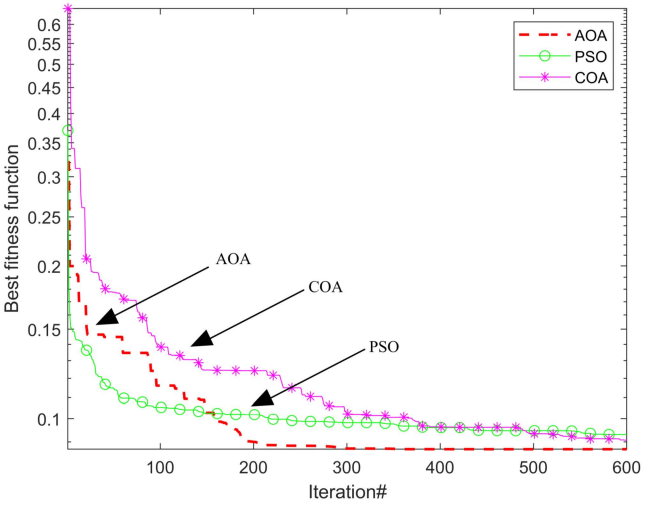

(d) Case 4

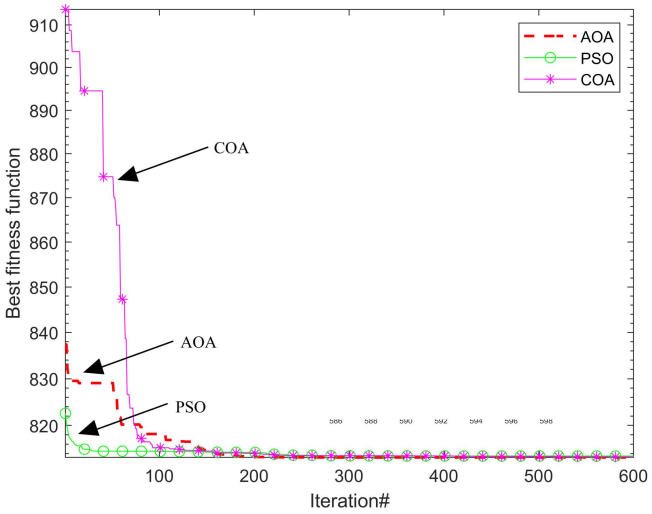

(e) Case 5

Fig. 2 Convergence of AOA on different cases.

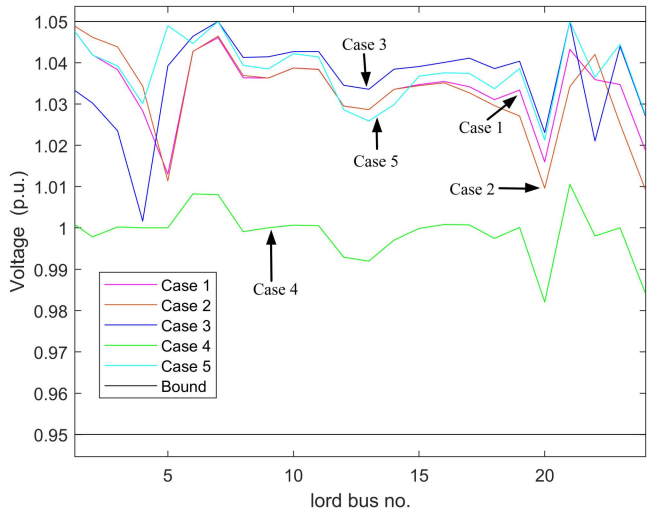

Fig. 3 Load bus voltage obtained by AOA.

TABLE 3. SIMULATION DATA OF AOA AND OTHER ALGORITHMS

Case#	Algorithm	Min	Max	Mean
Case 1	AOA	800.5005	800.6442	800.5379
	PSO	800.5587	800.6922	800.596
	COA	800.5382	802.8041	801.0338
	ABC [17]	800.6600	801.8674	800.8715
	MDE [8]	802.3760	802.404	802.382
	ARCBBO [18]	800.5159	800.9262	800.6412
Case 2	AOA	3.1282	3.1906	3.1510
	PSO	3.1580	3.9711	3.3627
	COA	3.0982	3.3383	3.1777
	ABC [17]	3.1078	-	-
	EGA [19]	3.2008	-	-
Case 3	AOA	0.1252	0.1263	0.1256
	PSO	0.1265	0.1293	0.1276
	COA	0.1258	0.1280	0.1267
	ABC [17]	0.1474	0.2607	0.1659
	ARCBBO [18]	0.1383	0.1398	0.1387
Case 4	AOA	0.0871	0.0959	0.0927
	PSO	0.0931	0.1202	0.1095
	COA	0.0907	0.1113	0.1028
	GSA [20]	0.0932	0.0941	0.0939
	ARCBBO [18]	0.0920	0.1257	0.1008
Case 5	AOA	813.1831	813.3971	813.3074
	PSO	813.4814	815.5348	814.0152
	COA	813.2884	813.5245	813.41
	MSA[21]	814.9378	-	-
	MDE[21]	815.8431	-	-

TABLE 4. EXPERIMENTAL DATA OF BEST SOLUTIONS FOR IEEE 30-BUS SYSTEM

Parameters	Case 1	Case 2	Case 3	Case 4	Case 5
P_{G_2} (MW)	48.9192	79.2802	60.3166	61.0641	48.7878
P_{G_5} (MW)	21.4707	49.9820	43.2761	48.0061	21.8111
P_{G_8} (MW)	21.4947	34.9994	28.0658	26.3729	21.6289
$P_{G_{11}}$ (MW)	12.0424	29.9987	26.8969	23.1373	11.9819
$P_{G_{13}}$ (MW)	11.1497	39.6528	35.4149	18.8282	10.8633
V_{G_1} (p.u.)	1.0832	1.0640	1.0505	1.0176	1.0835
V_{G_2} (p.u.)	1.0629	1.0594	1.0322	1.0108	1.0645
V_{G_5} (p.u.)	1.0323	1.0391	0.9894	1.0191	1.0353
V_{G_8} (p.u.)	1.0382	1.0445	1.0220	1.0039	1.0372
$V_{G_{11}}$ (p.u.)	0.9977	0.9969	1.0432	0.9891	1.0465
$V_{G_{13}}$ (p.u.)	1.0414	1.0405	1.0700	0.9954	1.0434
T_{11} (p.u.)	1.0661	1.0765	0.9992	1.0021	0.9789
T_{12} (p.u.)	0.9249	0.9111	1.0189	0.9864	1.0854
T_{15} (p.u.)	0.9780	0.9853	1.0108	0.9637	0.9674
T_{36} (p.u.)	0.9844	0.9984	0.9644	0.9744	0.98
$Q_{C_{10}}$ (MVAr)	4.6769	3.1566	3.8763	3.3251	4.9374
$Q_{C_{12}}$ (MVAr)	4.6588	4.6735	2.5747	4.9853	4.8513
$Q_{C_{15}}$ (MVAr)	.2885	4.9916	4.9718	4.9972	3.4579
$Q_{C_{17}}$ (MVAr)	3.8642	3.9916	4.9943	0.2422	4.9724
$Q_{C_{20}}$ (MVAr)	4.3146	4.4013	4.8912	3.5017	0.0815
$Q_{C_{21}}$ (MVAr)	4.9475	4.9968	4.9156	4.3211	4.9599
$Q_{C_{23}}$ (MVAr)	3.3323	2.6395	4.0754	4.7998	4.0995
$Q_{C_{24}}$ (MVAr)	2.9625	3.7683	4.8554	3.8671	2.2115
$Q_{C_{29}}$ (MVAr)	3.7594	3.6182	4.6190	3.1971	4.8073
P_{G_1} (MW)	177.3789	52.6179	94.1231	111.6118	177.3757
Fuel cost	**800.5005**	967.6906	844.4492	859.1888	**800.5628**
P_{loss} (MW)	9.0686	**3.1282**	6.3127	6.0241	9.0694
L-index(max)	0.1275	0.1281	**0.1252**	0.1396	**0.1262**
VD(p.u.)	0.9044	0.8509	0.9607	**0.0871**	0.9485

VI. Conclusions

In this paper, AOA is used to solve the optimal power flow problem for the IEEE-30 bus system, and the algorithm successfully achieves the goal of minimum power generation cost, minimum active power loss, minimum voltage stability and minimum bus voltage offset. AOA shows better astringency and robustness in the simulation experiments, and it can be used as an effective alternative technique to solve the OPF problem.

References

[1] S. Li, W. Gong, L. Wang, X. Yan, and C. Hu, "Optimal Power Flow by Means of Improved Adaptive Differential Evolution," *Energy*, vol. 198, pp. 117314, 2020.

[2] M. Huneault, and F. D. Galiana, "A Survey of the Optimal Power Flow Literature," *IEEE Transactions on Power Systems*, vol. 6, no. 2, pp. 762-770, 1991.

[3] J. A. Momoh, R. Adapa, and M. E. El-Hawary, "A Review of Selected Optimal Power Flow Literature to 1993. I. Nonlinear and Quadratic Programming Approaches," *IEEE Transactions on Power Systems*, vol. 14, no. 1, pp. 96-104, 1999.

[4] J. A. Momoh, M. E. El-Hawarym, and R. Adapa, "A Review of Selected Optimal Power Flow Literature to 1993. II. Newton, Linear Programming and Interior Point Methods," *IEEE Transactions on Power Systems*, vol. 14, no. 1, pp. 105-111, 1999.

[5] A. Meng, C. Zeng, P. Wang, D. Chen, and H. Yin, "A High-performance Crisscross Search Based Grey Wolf Optimizer for Solving Optimal Power Flow Problem," *Energy*, vol. 225, pp. 120211, 2021.

[6] Nadimi-Shahraki, Mohammad H., Shokooh Taghian, Seyedali Mirjalili, Laith Abualigah, Mohamed Abd Elaziz, and Diego Oliva, "EWOA-OPF: Effective Whale Optimization Algorithm to Solve Optimal Power Flow Problem," *Electronics*, vol. 10, no. 23: pp. 2975. 2021.

[7] P. P. Biswas, P. N. Suganthan, R. Mallipeddi, and G. Amaratunga, "Optimal Power Flow Solutions Using Differential Evolution Algorithm Integrated with Effective Constraint Handling Techniques," *Engineering Applications of Artificial Intelligence*, vol. 68, pp. 81-100, 2018.

[8] S. Sayah, and K. Zehar, "Modified Differential Evolution Algorithm for Optimal Power Flow with Non-smooth Cost Functions," *Energy Conversion and Management*, vol. 49, no. 11, pp. 3036-3042, 2008.

[9] E. E. Elattar, and S. K. ElSayed , "Modified JAYA Algorithm for Optimal Power Flow Incorporating Renewable Energy Sources Considering the Cost, Emission, Power Loss and Voltage Profile Improvement," *Energy*, vol. 178, pp. 598-609, 2019.

[10] J. Zhang, Q. Tang, Y. Chen, and S. Lin, "A hybrid Particle Swarm Optimization with Small Population Size to Solve the Optimal Short-term Hydro-thermal Unit Commitment Problem," *Energy*, vol. 109, pp. 765-780, 2016.

[11] B. Mahdad, and K. Srairi, "Security Constrained Optimal Power Flow Solution Using New Adaptive Partitioning Flower Pollination Algorithm," *Applied Soft Computing*, vol. 46, pp. 501-522, 2016.

[12] B. Bentouati, H. R. E. H. Javaid, A. A. Bouchekara, El-Fergany, and S. Arabia, "Optimizing Performance Attributes of Electric Power Systems Using Chaotic Salp Swarm Optimizer," *International Journal of Management Science and Engineering Management*, vol. 15, no. 3, pp. 165-175, 2020.

[13] F. A. Hashim, K. Hussain, E. H. Houssein, M. S. Mabrouk, and W. Al-Atabany, "Archimedes Optimization Algorithm: a New Metaheuristic Algorithm for Solving Optimization Problems," *Applied Intelligence*, vol. 51, no. 3, pp. 1531-1551, 2021.

[14] Y. Li, H. Zhu, D. Wang, K. Wang, and X. Wu, "Comprehensive Optimization of Distributed Generation Considering Network Reconstruction Based on Archimedes Optimization Algorithm," *IOP Conference Series: Earth and Environmental Science*, vol. 647, pp. 012031, 2021.

[15] L. Zhang, J. Wang, X. Niu, and Z. Liu, "Ensemble Wind Speed Forecasting with Multi-objective Archimedes Optimization Algorithm and Sub-model Selection," *Applied Energy*, vol. 301, pp. 117449, 2021.

[16] A. Fathy, A. G. Alharbi, S. Alshammari, and H. M. Hasanien, "Archimedes Optimization Algorithm Based Maximum Power Point Tracker for Wind Energy Generation System," *Ain Shams Engineering Journal*, vol. 13, no. 2, pp. 101548, 2022.

[17] M. R. Adaryani, and A. Karami, "Artificial Bee Colony Algorithm for Solving Multi-objective Optimal Power Flow Problem," *International Journal of Electrical Power & Energy Systems*, vol. 53, pp. 219-230, 2013.

[18] A. R. Kumar, and L. Premalatha, "Optimal Power Flow for a Deregulated Power System Using Adaptive Real Coded Biogeography-based Optimization," *International Journal of Electrical Power & Energy Systems*, vol. 73, pp. 393-399, 2015.

[19] M. Sailaja Kunari, and S. Maheswarapu, "Enhanced Genetic Algorithm Based Computation Technique for Multi-objective Optimal Power Flow," *International Journal of Electrical Power & Energy Systems*, vol. 32, no. 6, pp. 736-742, 2010.

[20] S. Duman, U. Güvenç, Y. Sönmez, and N. Yörükeren, "Optimal Power Flow Using Gravitational Search Algorithm,"*Energy Conversion and Management*, vol. 59, pp. 86-95, 2012.

[21] A. A. A. Mohamed, Y. S. Mohamed, A. A. El-Gaafary, and A. M. Hemeida, "Optimal Power Flow Using Moth Swarm Algorithm," *Electric Power Systems Research*, vol. 142, pp. 190-206, 2017.